

# Correlation function for the Grid-Poisson Euclidean matching on a line and on a circle

Elena Boniolo \*

*Dipartimento di Fisica dell'Università degli Studi di Milano*  
*via Celoria 16, I-20133 Milano, ITALY*  
elena.boniolo@gmail.com

Sergio Caracciolo

*Dipartimento di Fisica dell'Università degli Studi di Milano, and INFN,*  
*via Celoria 16, I-20133 Milano, ITALY*  
Sergio.Caracciolo@mi.infn.it

Andrea Sportiello

*LIPN, and CNRS, Université Paris 13, Sorbonne Paris Cité,*  
*99 Av. J.-B. Clément, 93430 Villetaneuse, FRANCE*  
Andrea.Sportiello@lipn.fr

October 8, 2018

## Abstract

We compute the two-point correlation function for spin configurations which are obtained by solving the Euclidean matching problem, for one family of points on a grid, and the second family chosen uniformly at random, when the cost depends on a power  $p$  of the Euclidean distance. We provide the analytic solution in the thermodynamic limit, in a number of cases ( $p > 1$  open b.c. and  $p = 2$  periodic b.c., both at criticality), and analyse numerically other parts of the phase diagram.

---

\*Actual address: School of Physics, HH Wills Physics Laboratory, University of Bristol, Tyndall Avenue, Bristol, BS8 1TL, United Kingdom

# 1 Introduction

## 1.1 The problem

The *Matching Problem* is an optimisation problem, in which the set of feasible configurations consists of possible maximal matchings in a bipartite graph, and the cost function is the sum of the costs on the individual chosen edges.

Let us call  $\mathcal{K}_{N,M}$  the complete bipartite graph, so that the set of vertices  $V$  is partitioned in  $V = \mathcal{R} \cup \mathcal{B}$ , where  $\mathcal{R} = \{r_1, \dots, r_N\}$  is the set of *red* vertices, and  $\mathcal{B} = \{b_1, \dots, b_M\}$  is the set of *blue* vertices.

Assume, without loss of generality at this point, that  $N \leq M$ . Maximal matchings are thus the set  $\Pi$  of injective mappings  $\{\pi : \mathcal{R} \rightarrow \mathcal{B}\}$ . Given a collection of *weights*  $w(r_i, b_j) = w(i, j) \in \mathbb{R}^+ \cup \{+\infty\}$ , we assign to each maximal matching  $\pi \in \Pi$  the cost  $E(\pi)$  defined as

$$E(\pi) = \sum_{i=1}^N w(i, \pi(i)). \quad (1)$$

The *optimal* matching  $\pi_{\text{opt}}$ , and optimal cost  $E_{\text{opt}}$ , are the quantities that realize the minimum cost

$$E_{\text{opt}} = E(\pi_{\text{opt}}) = \min_{\pi \in \Pi} E(\pi). \quad (2)$$

This problem models a variety of concrete applications in Optimisation Theory. In particular, it is the discrete version of a problem introduced by Monge [1], back in 1781, where blue and red sites corresponded to production and exploitation sites of some resource, and the matching is optimising the cost of transportation. The continuous version of the problem, in which one has to find the mapping which minimises the transport condition between two given measures (the red and the blue ones) is also of relevance and is studied under the name of Monge–Kantorovič problem [2].

The research of the optimal matching in a bipartite weighted graph is usually called the *Assignment Problem*. Both the bipartite and non-bipartite optimal matching problems are of polynomial complexity, and the bipartite case has a considerably simpler algorithm.

A classical polynomial algorithm for the Assignment Problem is due to Kuhn [3], who called it *Hungarian Algorithm* as a tribute to the country of origin of the authors of the two main lemmas on which it is based, Kőnig and Egerváry. As reported by Knuth [4], after the work of Munkres [5] for speeding up a certain ‘recovering procedure’, the complexity is cubic in  $M$ .

Questions of statistical nature arise when the set of weights are stochastic variables, and the optimal quantities  $\pi_{\text{opt}}$  and  $E_{\text{opt}}$  are analysed probabilistically. In

particular, we are motivated to consider these problems because of the close connection between random optimization problems and the statistical mechanics of disordered systems [6–10]. Indeed, when the weights  $w(i, j)$  are equally distributed independent random variables, drawn from a large range of single-weight distributions, by using the celebrated *replica trick*, Mezárđ and Parisi could compute the average cost for both the matching on the complete graph [11], the *random matching problem*, and on the complete bipartite graph [12], the *random bipartite matching problem*. See [13] for a derivation without replicas.

## 1.2 Considerations at generic dimension $d$

The fact that the weights are equally distributed implies, in particular, that the stochastic problem has no underlying finite-dimensional geometry, i.e. it is a *spherical*, or *mean-field* disordered problem. The implementation of the model we are going to discuss, named the *Grid-Poisson matching problem*, is instead naturally embedded in a finite dimension  $d$ .

In this paper we will be mainly concerned with the (much simpler) case  $d = 1$ . However, in this introduction we supply a number of observations in the case of generic  $d$ .

For  $L$  an integer, define the box  $\Lambda = [0, L]^d \subset \mathbb{R}^d$ . The set of red vertices  $\mathcal{R}$  is chosen to be  $\mathcal{R} = \Lambda \cap (\mathbb{Z} + \frac{1}{2})^d$ , i.e. the set of  $N = L^d$  points within  $\Lambda$  that have all semi-integer coordinates. The set of blue vertices,  $\mathcal{B}$ , is a set of  $M$  points chosen uniformly at random in  $\Lambda$ . Introducing a further parameter  $p > 0$ , the weight is taken to be the corresponding power of the Euclidean distance  $d(i, j)$  between  $r_i$  and  $b_j$

$$w(i, j) = (d(i, j))^p \quad (3)$$

In such a case, we say that we have *open boundary conditions*. In the variant in which  $\Lambda$  is compactified on a torus, and  $d(i, j)$  is the minimal distance among the translation images,<sup>1</sup> we say that we have *periodic boundary conditions*.

The case of main interest is  $p = 1$ , where the total cost has a direct pictorial interpretation as the total length of the segments. It is also the value at which the function  $x \rightarrow x^p$  changes its behaviour (it is concave for  $0 < p < 1$ , and convex for  $p > 1$ ), a property of relevance for the problem at hands. The cases of  $p$  an even integer are also special, as the Euclidean distance to the power  $p$  can be expressed as a polynomial in the Cartesian coordinates of the points.

A related model, the *Poisson-Poisson matching problem*, where both the red and blue sets occur as independent Poisson processes of equal intensity, has been considered in [14–16]. The *Euclidean monopartite matching problem* has also been

---

<sup>1</sup>I.e., in such a case,  $d((x_1, \dots, x_d), (y_1, \dots, y_d)) = \min_{\nu \in \mathbb{Z}^d} \sqrt{\sum_{a=1}^d (y_a - x_a - \nu_a L)^2}$ .

studied by using the replica trick [12], by taking corrections to the random matching problem. The *minimax Grid-Poisson matching problem* has been studied in [18–20]. In this problem, the cost function is changed from (1) into

$$E^{\text{m.m.}}(\pi) = \max_{1 \leq i \leq N} w(i, \pi(i)). \quad (4)$$

It is easy to see that this problem is a limit  $p \rightarrow +\infty$  of the class of problems defined above, namely, for the same set of points,  $\pi_{\text{opt}}^{\text{m.m.}} = \lim_{p \rightarrow \infty} \pi_{\text{opt}}^{(p)}$  and  $E_{\text{opt}}^{\text{m.m.}} = \lim_{p \rightarrow \infty} (E_{\text{opt}}^{(p)})^{\frac{1}{p}}$ .

In a generic configuration of points, each red point  $r_i$  has a unique nearest blue point  $b_{j(i)}$ , and vice versa. If  $j(i) \neq j(i')$  for all  $i \neq i'$ , the corresponding matching is easily certified to be optimal, for all values of  $p$  simultaneously. Such a simple situation occurs with increasing probability for  $M/N \rightarrow \infty$ , and, in a symmetric way exchanging red and blue, for  $M/N \rightarrow 0$ . Conversely, when  $N \sim M$  we expect competing effects for the colliding pairs  $(i, i')$  such that  $j(i) = j(i')$ , analogous to frustration in disordered systems, and long-range correlations, of the order of the size of the system, may arise. For this reason, we shall look at the *continuum limit*, in which both  $N$  and  $M$  become infinitely large, by keeping fixed the ratio

$$\rho := \frac{M}{N}. \quad (5)$$

Let us say that  $\xi = \xi(\rho)$  is a scale of correlations in the system, at given density, and in the continuum limit. As it will turn out,  $\xi$  diverges at only one *critical* value of the density  $\rho^*$ , like in a second-order phase transition. Under this assumption, it is clear that, in the Poisson-Poisson problem,  $\rho^* = 1$ . This seems to remain numerically true, although theoretically more subtle, in the Grid-Poisson case.

An argument for justifying both the second-order character of the behaviour of  $\xi(\rho)$ , and the stability of the position of the critical density at the self-dual value, is through a coarse-grain analysis.

More generally, consider the case in which red and blue points arise from two independent processes, one of which being Poisson, the other one having fluctuations at most as in the Poisson case (it may be another Poisson process, or a regular lattice, or a Determinantal process, ...). Consider boxes in  $\Lambda$  of size  $X = v^{\frac{1}{d}}$ , and assume that  $1 \ll X \ll L$ . The average number of red and blue points are  $v$  and  $\rho v$ , respectively. The fluctuations on these numbers are of the order of  $\sqrt{v}$ . As soon as  $\sqrt{v} > \frac{1}{|\rho-1|}$ , with large probability there are enough blue points within each box to be matched to the red points. Thus, the matching obtained by solving the problem separately in each box is maximal, and has all edges of length bounded by  $\sim v^{\frac{1}{d}}$ . Conversely, if  $\rho = 1$ , at all coarse-grain scales we will have important fluctuations. A first coarse-graining at scale  $v^{\frac{1}{d}}$  will leave  $\sim \sqrt{v}$  unmatched red or blue points

per box, independently on each box. A further coarse-graining at scale  $(kv)^{\frac{1}{d}}$ , for the remaining points, gives around  $kv^{\frac{1}{2}}$  points of each colour, and around  $k^{\frac{1}{2}}v^{\frac{1}{4}}$  excess of points of one colour, thus a feature analogous to a single coarse-graining at scale  $(k\sqrt{v})^{\frac{1}{d}}$ . The self-similarity of the coarse-graining procedure is a signature of an interesting behaviour under the group of renormalisation, and of long-range correlations.

For these reasons, we predict that, also in the Grid-Poisson case the critical density is for  $\rho = 1$ , and set

$$t := \rho - 1 \tag{6}$$

as a useful shortcut for the *reduced temperature*, which vanishes at the critical point.

Our aim is to study the correlations which emerge in the *scaling region* around the critical point.

### 1.3 Observables

As we have chosen to sample red and blue points through two distinct procedures, we no longer have a symmetry of the problem under exchange of red and blue points. Thus in the case  $N \leq M$  the maximal matchings are injections from  $\mathcal{R}$  to  $\mathcal{B}$ , and in the case  $N \geq M$  the maximal matchings are injections from  $\mathcal{B}$  to  $\mathcal{R}$ . (Of course, for  $M = N$  we have bijections, i.e. permutations.)

Let  $r_i$ , with  $i = 1, \dots, N$  be the vector of integer coordinates for the red points and  $b_j$ , with  $j = 1, \dots, M$ , the vector of real coordinates for the blue points. We define a collection of  $\min(N, M)$  vectors  $\varphi_i$  associated to the red points covered by the optimal matching. If  $(i, j)$  is an edge in  $\pi_{\text{opt}}$ , we set

$$\varphi_i := b_j - r_i \tag{7}$$

In particular,

$$E_{\text{opt}} = \sum_{i=1}^{\min(N, M)} |\varphi_i|^p. \tag{8}$$

The quantities  $\varphi_i$  behave as  $O(d)$  vectors on the lattice. As for  $O(n)$  models in (non-disordered) statistical mechanics systems, we expect that the spontaneous symmetry breaking, if any, occurs in the angular degrees of freedom. For this reason we also introduce, for the same set of indices  $i$ , a *spin variable*  $\sigma_i$

$$\sigma_i := \frac{\varphi_i}{|\varphi_i|} \tag{9}$$

Let  $\sigma_i = 0$  if  $M < N$ , and  $i$  is not covered in the optimal matching.

Thus, a model, here given by a triple  $(d, L, p)$ , induces a measure  $\mu(\sigma)$  over the corresponding set of spin variables. We shall characterize the critical behaviour of our model by looking at the correlation function

$$G(x, y) := \sum_{\sigma} \mu(\sigma) \sigma_x \cdot \sigma_y = \langle \sigma_x \cdot \sigma_y \rangle \quad (10)$$

with  $x, y$  points of our grid.

At this point, an advantage of the Grid-Poisson version of the problem, w.r.t. the Poisson-Poisson version, becomes evident. The statistical properties of  $G(x, y)$  are more easily investigated numerically in the first case, in particular for periodic boundary conditions, where  $G(x, y) = G(y - x)$  takes as argument an integer-valued vector in  $\mathbb{Z}^d$ , instead of a real-valued vector.

Define the correlation function averaged over pairs of points with the same distance

$$G(r; L, t) = \frac{\sum_{(x,y):d(x,y)=r} G(x, y)}{\sum_{(x,y):d(x,y)=r} 1}. \quad (11)$$

In the region near criticality we expect *finite-size scaling* of the correlation functions. In particular for the two-point function in (11), this means that it must be a homogeneous function of its arguments, according to

$$G(r; L, t) = L^{\alpha} F\left(\frac{r}{L}, t L^{\frac{1}{\nu}}\right) \quad (12)$$

where the exponents  $\alpha$  and  $\nu$  and the function  $F$  are *universal*, that is are common to other models in the same universality class. In particular, for our family of models, we expect them to depend on the dimensionality  $d$ , and the exponent  $p$  by which the Euclidean distance enters the cost function. In this paper they will be the main argument of our interest.

We repeat that in this paper we study the one-dimensional version of the problem, in the two variants of boundary conditions, open and periodic.

## 2 Open boundary conditions

In this section we analyse the one dimensional Matching Problem with open boundary conditions.

### 2.1 Properties of the optimal matching

We start from analysing some general properties of the problem on a line with open boundary conditions.

We first discuss the consequences of the choice of the exponent  $p$  which appears in the weights (3). Let us compare the cost of matchings such that two given red points  $r_1, r_2$  are matched to two given blue points  $b_1, b_2$  (in one of the two orders), given that the rest of the configuration is the same. If we determine which of the two orders is the best, we have a criterion for excluding that the other ordering is part of the optimal matching. The analysis goes through a case study, for the  $4! = 24$  possible orderings of  $\{r_1, r_2, b_1, b_2\}$  along the line. Of course, the discrete symmetries reduce the analysis to only three cases, that we denote by the pictograms  $[\bullet\bullet\circ\circ]$ ,  $[\bullet\circ\circ\circ]$  and  $[\bullet\circ\circ\bullet]$ .

Let  $T_1$  be the cost of the matching in which the leftmost red point goes with the leftmost blue one, and  $T_2$  the cost of the other possible matching. We shall call the first case *ordered*. More generally, we shall call *ordered* a matching such that, for all pairs of edges  $(r_1, b_1), (r_2, b_2)$ , if  $r_1 < r_2$  then  $b_1 < b_2$ . If we draw a matching with arcs on the upper half-plane, some of the arcs may cross. We call a matching *crossing* if this occurs, and *non-crossing* otherwise.

**First case,  $[\bullet\bullet\circ\circ]$ .** Let the positions be, from left to right,  $z, z + y, z + y + x_1, z + y + x_2$  with  $x_2 > x_1$  (see Fig. 1). As the distances are invariant under translations we can choose  $z = 0$  and we can also set  $y = 1$ , by choosing the unit of lengths.

The first matching is ordered, the second one is non-crossing. The costs of the two matchings are

$$T_1 = (1 + x_1)^p + x_2^p \quad (13)$$

$$T_2 = (1 + x_2)^p + x_1^p. \quad (14)$$

Now,  $T_1 \leq T_2$  if and only if

$$(1 + x_1)^p - x_1^p \leq (1 + x_2)^p - x_2^p \quad (15)$$

The function  $f(x) = (1 + x)^p - x^p$  is always increasing, respectively decreasing, on  $\mathbb{R}^+$ , when  $p > 1$ , respectively  $p < 1$  (and is  $f(x) = 1$  for  $p = 1$ ).

Thus, for  $p > 1$  the ordered matching has a lower cost. For  $p = 1$  the two matchings have the same cost. For  $p < 1$  the non-crossing matching has lower cost.

**Second case,  $[\bullet\circ\circ\circ]$ .** Similarly to the case above, by translating and scaling we can get rid of two parameters. Let the positions be  $0, 1 - x_1, 1, 1 + x_2$  with  $0 < x_1 < 1$ . In this case, the two possible matchings are both non-crossing. The costs are now

$$T_1 = (1 - x_1)^p + x_2^p \quad (16)$$

$$T_2 = (1 + x_2)^p + x_1^p. \quad (17)$$

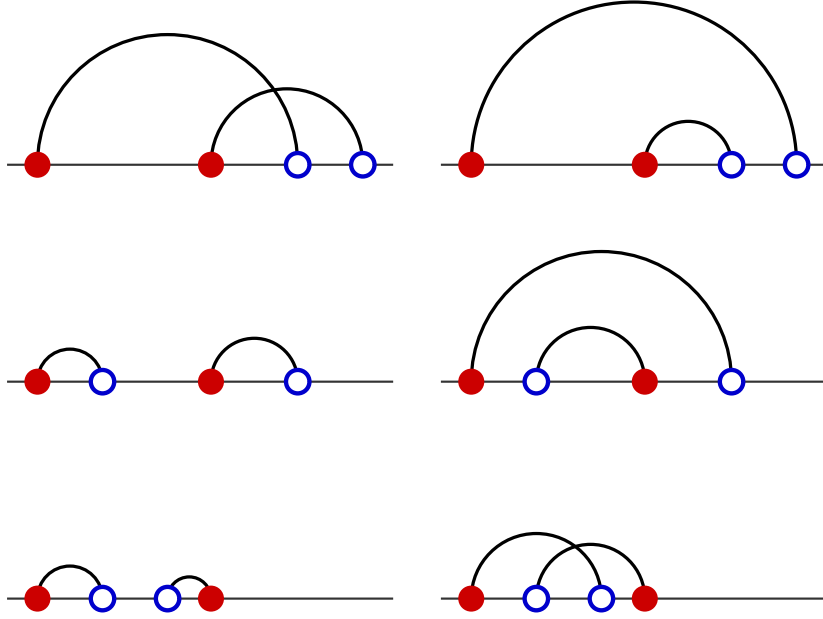


Figure 1: Matchings for size-2 instances. Each line corresponds to a particular disposition of the blue points. The matchings on the left are all *ordered*. The first and the last matching are *crossing*.

Now,  $T_1 \leq T_2$  if and only if

$$(1 - x_1)^p - x_1^p \leq (1 + x_2)^p - x_2^p. \quad (18)$$

For  $p \geq 1$  this is always true, because

$$(1 - x_1)^p - x_1^p \leq 1 \leq (1 + x_2)^p - x_2^p \quad (19)$$

which implies that the ordered matching has a lower cost.

For  $p < 1$ , at fixed  $x_2$ , the ordered matching has a lower cost only for a range of values  $x_1$ . For example, let  $p = 1/2$  and set  $z = \sqrt{1 + x_2} - \sqrt{x_2}$ , which maps the domain  $x_2 \in [1, \infty)$  into  $z \in (0, 1]$ . Then the ordered matching has a lower cost if and only if

$$x_1 > \frac{1}{2} \left( 1 - \sqrt{2z^2 - z^4} \right) \quad (20)$$

which does *not* cover the full domain  $x_1 \in [0, 1]$ , in general.

**Third case,  $[\bullet \circ \circ \bullet]$ .** Let the positions be  $0, x_1, x_2, 1$  with  $0 < x_1 < x_2 < 1$ . In this case the ordered matching is non-crossing, the other one is crossing. The

costs are now

$$T_1 = x_1^p + (1 - x_2)^p \tag{21}$$

$$T_2 = x_2^p + (1 - x_1)^p . \tag{22}$$

Now,  $T_1 \leq T_2$  if and only if

$$x_1^p - (1 - x_1)^p \leq x_2^p - (1 - x_2)^p \tag{23}$$

which is always the case for  $p \geq 0$  because the function  $f(x) = x^p - (1 - x)^p$  is increasing on  $[0, 1]$ .

From this analysis we deduce the following two statements.

**Proposition 2.1** *For  $p > 1$  the optimal matching is ordered. For  $p < 1$  the optimal matching is non-crossing. For  $p = 1$  there exists an optimal matching which is ordered, and one which is non-crossing.*

**Proof.** Assume by absurd that the optimal matching is not ordered, and consider a pair of edges  $(r_1, b_1)$ ,  $(r_2, b_2)$  which certify this. From the previous analysis we see that by re-ordering them we obtain a cost which is strictly lower (resp. weakly lower) for  $p > 1$  (resp. for  $p = 1$ ). The argument for the non-crossing statement is analogous.  $\square$

Let us remark that when  $N = M$ , that is where we expect criticality, and when  $p > 1$ , the solution of the matching problem is very simple because there is only one ordered matching.<sup>2</sup> Since we are on a line, we can label red and blue points in increasing order. The solution of the matching problem is the one in which the  $i$ -th red point is associated with the  $i$ -th blue point. Then  $\varphi_i = b_i - r_i$  and  $\sigma_i = \text{sgn } \varphi_i \in \{-1, 1\}$  is the Ising spin variable that we can associate with the solution. Furthermore, as  $\pi_{\text{opt}}$  does not change in the full range  $p > 1$ , all the geometric quantities (and in particular the variables  $\sigma_i$ ) are studied simultaneously for all  $p$  in this range. For definiteness, we shall take  $p = 2$  as our preferential case in this range, as, in the case of periodic boundary conditions, for this value we have an important simplification.

When  $p = 1$ , almost surely on any optimal matching there is a finite fraction of pairs of edges, with neighbouring red indices, in the pattern  $[\bullet\bullet\circ\circ]$ . This suggests that almost surely there is a large degeneracy of the optimal configuration.

---

<sup>2</sup>The analogous statement, for  $p < 1$  and non-crossing matchings, does not hold because the pattern  $[\bullet\circ\bullet\circ]$  has two potentially good non-crossing pairings.

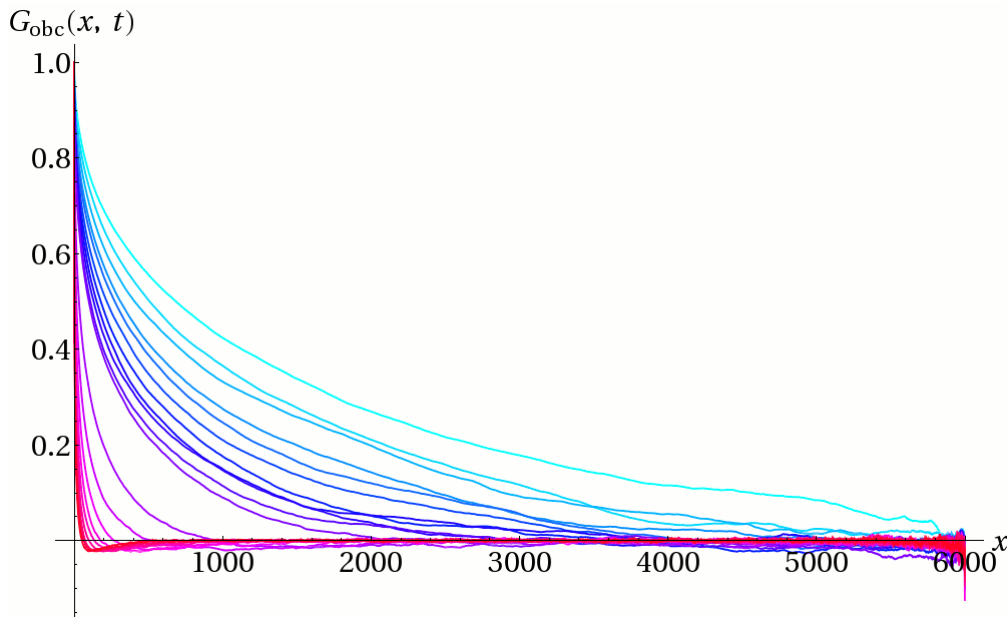


Figure 2: The correlation function with open boundary conditions at size 6000. From cyan to purple,  $t = 0, 0.001, 0.002, 0.003, 0.004, 0.005, 0.006, 0.007, 0.008, 0.009, 0.01, 0.02, 0.03, 0.04, 0.05, 0.06, 0.07, 0.08, 0.09, 0.1$ .

## 2.2 Numerical results

We begin from the case  $p = 2$ .

In Fig. 2 we report the correlation function  $G(r; L, t)$  for various choices of the parameter  $t$  when the size of the system is  $L = 6000$ . Each curve is the mean over  $10^3$  instances for the positions of the blue points. Of course, The shape of the functions for the corresponding negative values of  $t$  are undistinguishable.

We notice that  $G(r; L, t)$  presents two ranges of behaviour. If  $|t| < \bar{t}(L)$  (with  $\bar{t}(L) \approx 0.01$  when  $L = 6000$ ) the function is strictly positive, it is decreasing with  $r$ , and has, therefore, a minimum at  $r = L$ . On the other hand, if  $|t| > \bar{t}(L)$ , the shape is different. It reaches a minimum at an intermediate value  $r'$ , then goes up again approaching zero as  $r \rightarrow L$ . Whenever finite-size scaling holds for the two-point function (12), for large  $L$ , we get that  $\bar{t}(L)L^{\frac{1}{\nu}}$  is constant.

In Fig. 3 we show the correlation functions at criticality for various sizes. In this case each numerical point has been obtained by using  $10^4$  instances for the positions of the blue points. All curves are trivially mapped one onto the others by the simple rescaling  $r \rightarrow r/L$ . That is

$$G(r; L, 0) = G\left(\frac{r}{L}\right). \quad (24)$$

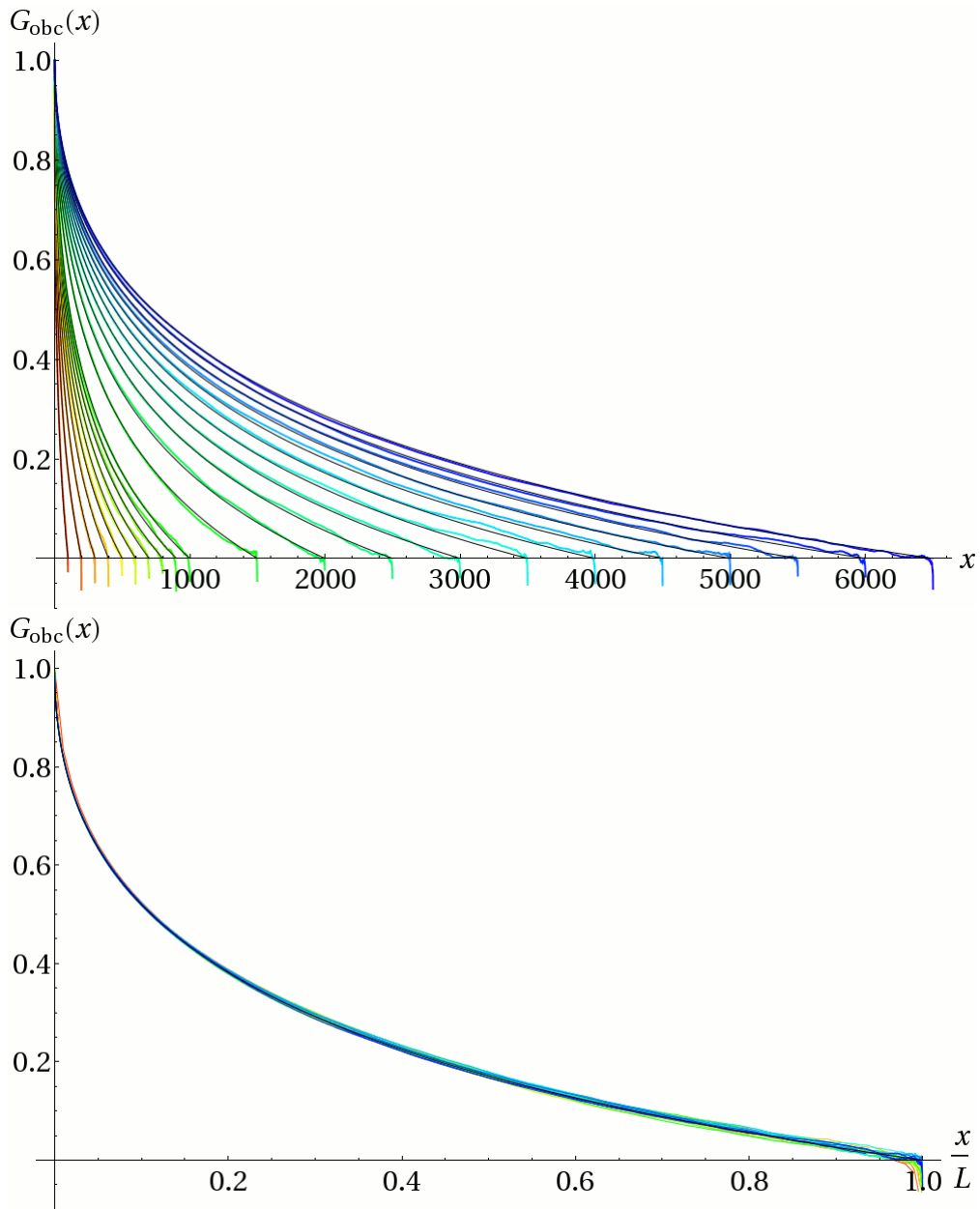


Figure 3: The correlation function at the critical point with open boundary conditions. Top: increasing sizes are represented from red ( $L = 100$ ) to blue ( $L = 6500$ ); Bottom: the same experimental curves, rescaled to show the agreement with the theoretical function, equation (57), regardless of the size.

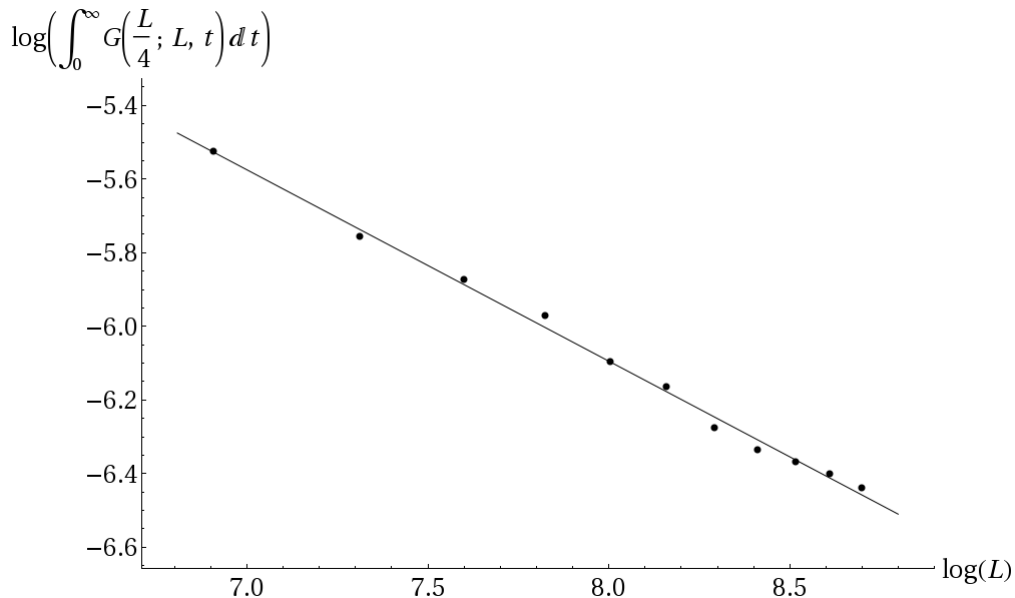


Figure 4:  $\log I(L/4, L)$ , defined by (25), for different values of  $L$ .

This means that in (12) we can set  $\alpha = 0$ .

In order to estimate the exponent  $\nu$ , notice that, if in the scaling region, that is  $|t| < \bar{t}(L)$ , the relation (12) holds, then

$$I(r, L) := L^{-\alpha} \int_0^{\bar{t}(L)} G(r; L, t) dt = L^{-\frac{1}{\nu}} \int_0^{\bar{t}(L) L^{\frac{1}{\nu}}} F\left(\frac{r}{L}, z\right) dz \quad (25)$$

$$\approx L^{-\frac{1}{\nu}} \int_0^\infty F\left(\frac{r}{L}, z\right) dz \quad (26)$$

because  $F$  vanishes rapidly with increasing  $z$ . As at fixed  $r/L$  the integral of  $F$  simply provides a constant, this expression shows a dependence on  $L$  which determines  $\nu$ .

In Fig. 4 we report the evaluation of  $\log I(r, L)$ , defined by (25), for different values of  $L$  at the point in which  $r = L/4$ . The integral has been evaluated through a polynomial interpolation in  $t$  among the numerical values we had determined. We find

$$\nu = 1.95 \pm 0.05 \quad (27)$$

In Fig. 5 we plot the correlation function at  $r = L/4$  as a function of  $\sqrt{L}t$ . All the points obtained from different values of  $L$ , large enough, and  $t$ , in the scaling region, fall, approximately, on the same curve.

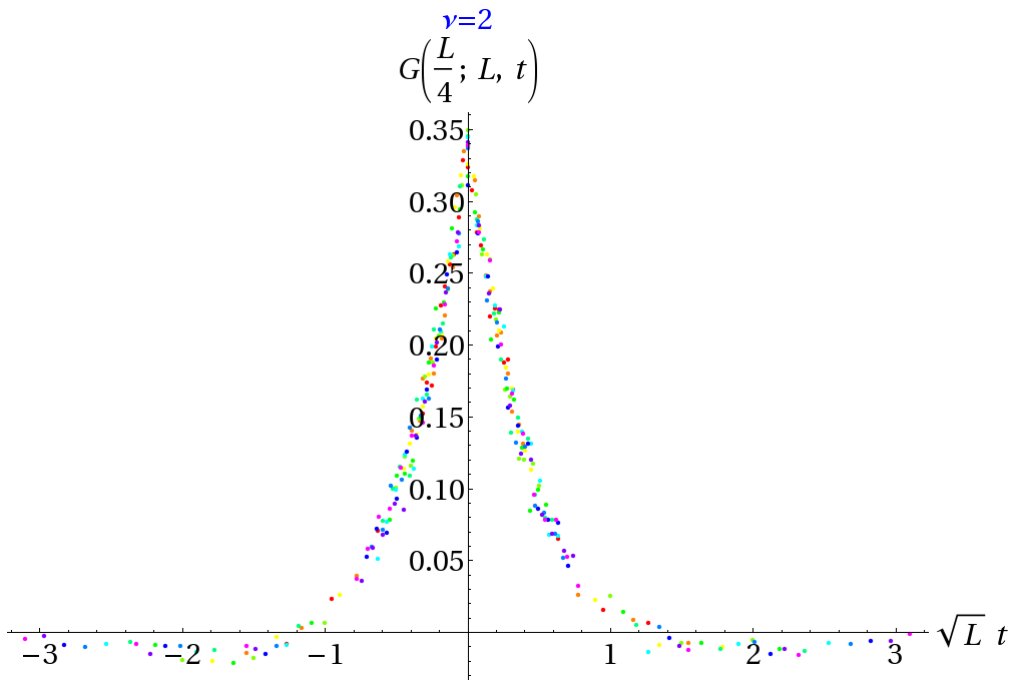


Figure 5: The correlation function from different values of  $L$  at  $t$  at  $r/L = 1/4$  as a function of  $\sqrt{L}t$ .

$p$	$-\alpha$
1	$0.00 \pm 0.03$
0.95	$0.08 \pm 0.04$
0.90	$0.18 \pm 0.04$
0.85	$0.28 \pm 0.04$
0.80	$0.37 \pm 0.04$
0.75	$0.47 \pm 0.04$

Table 1: Numerical estimates of the critical exponent  $\alpha$  in the region  $p < 1$ .

We have performed a similar analysis for the case  $p < 1$ , where, in contrast to the case  $p > 1$  there is no reason to expect that the values of the critical indices do not depend on  $p$ . Indeed, while we find always the same exponent  $\nu$ , the exponent  $\alpha$  shows the differences summarised in Table 1. The exponent  $\alpha$  has been computed by using the value of the two-point correlation function at distance  $r = L/4$  and the scaling ansatz (12) at criticality. We find approximately

$$\alpha \approx -2(1 - p) \quad (28)$$

in the region  $p \in [0.75, 1]$ .

### 2.3 Analytical predictions at criticality

Recall that, from the fact that the solution is ordered, we just have, for  $i = 1, \dots, L$

$$\varphi_i = b_i - r_i = b_i - i + \frac{1}{2}. \quad (29)$$

The collection of  $\varphi_i$ 's, for  $i$  labeled in order, can be transformed into a stochastic function from  $[0, 1]$  to  $\mathbb{R}$ , by setting  $\varphi(s) = \varphi_i$  for  $s \in [(i-1)/L, i/L]$ . The parameter  $s \in [0, 1]$  is a sort of *time* variable, for the evolution of a random walk.

Given that there are  $L$  blue points in the interval  $[0, L]$ , the probability to find the  $i$ -th blue point in the interval  $[y, y + dy]$  is given by

$$P_i(dy) = \frac{\frac{y^{i-1} (L-y)^{L-i}}{(i-1)! (L-i)!}}{\frac{y^L}{L!}} dy = \binom{L}{i} \left(\frac{y}{L}\right)^i \left(1 - \frac{y}{L}\right)^{L-i} \frac{i}{y} dy = B_i\left(L; \frac{y}{L}\right) \frac{i}{y} dy \quad (30)$$

where  $B_i(n; p)$  is the binomial distribution, for getting  $i$  ‘head’ when tossing  $n$  times a biased coin with probability  $p$  for ‘head’. In the limit of large  $L$ , by keeping fixed the ratio  $s = y/L$ , we get by the central limit theorem that

$$B_i(L; s) \rightarrow \frac{e^{-\frac{(i-y)^2}{2Ls(1-s)}}}{\sqrt{2\pi Ls(1-s)}} \quad (31)$$

which tells us that the difference  $i - y$  is of order  $\sqrt{L}$  so that by the change of variables

$$\varphi_i = \sqrt{L} x_i + \frac{1}{2} \quad (32)$$

we get the probability distribution

$$p_{B(s)}(x) = \frac{e^{-\frac{x^2}{2s(1-s)}}}{\sqrt{2\pi s(1-s)}} \quad (33)$$

which is the Gaussian probability distribution of a Brownian bridge  $B(s)$  over the interval  $[0, 1]$  (see Fig. 6). Precise definitions and further details can be found in Appendix A.

Essentially the same calculation can be performed for the joint probability distribution for displacements from different blue points to see that it always provides, in the limit of large  $L$ , the joint distribution at different times of a Brownian bridge.

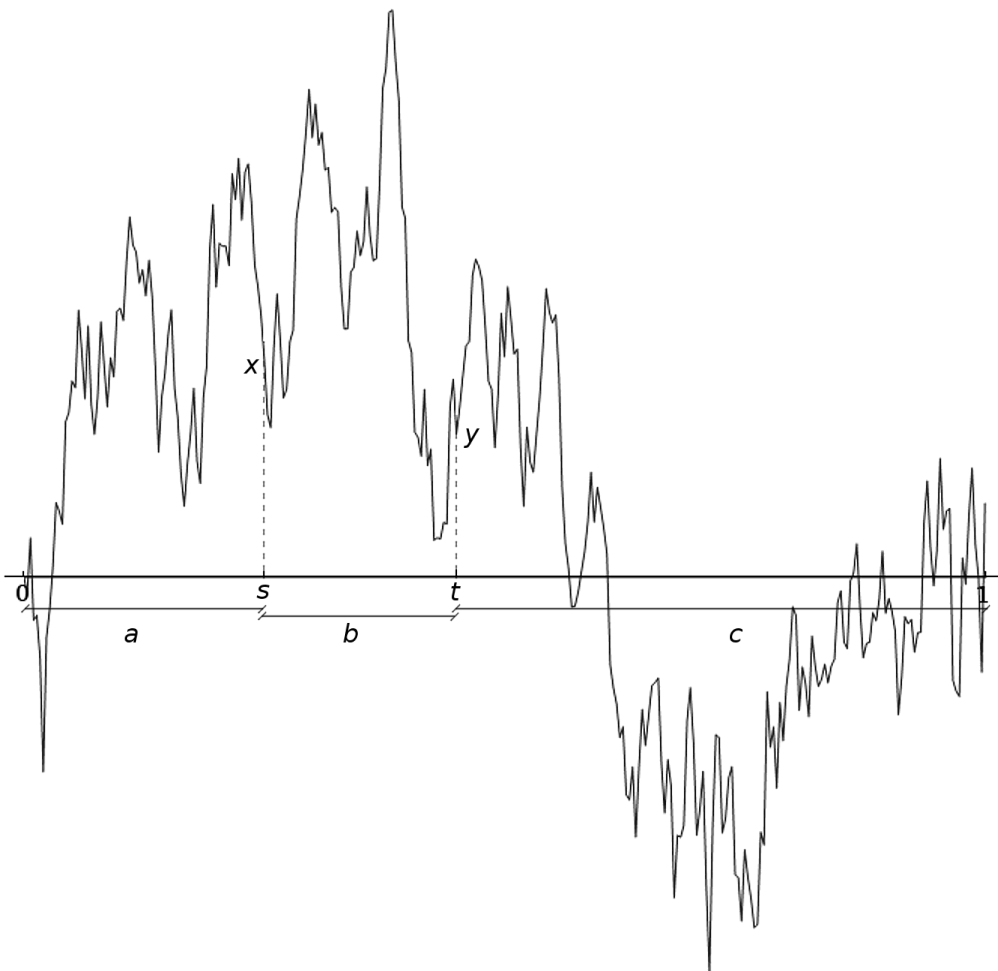


Figure 6: Schematic representation of a Brownian bridge  $B$  over the interval  $[0, 1]$ , and its value at the intermediate times  $s$  and  $t$ .

Remark that this result would remain unchanged for the Poisson-Poisson matching. In that case, also the red points would be distributed like the blue points, and the difference of two random variables distributed according to the same binomial distribution  $B(L; y/L)$  is still a binomial with distribution  $B(2L; y/L)$ . In order to converge to the same continuum limit we must rescale our variables as

$$\varphi_i = \sqrt{2L} x_i, \quad (34)$$

which explains the discrepancy, in certain factors 2, of our results w.r.t. analogous calculations, present in the literature, for the Poisson-Poisson case.

As a first consequence of the distribution function that we have obtained, we

can evaluate the cost of the optimal Grid-Poisson matching:

$$L^{-\frac{p}{2}} E_{\text{opt}} \rightarrow \int_0^1 ds \mathbb{E}(x^p(s)) = \int_0^1 ds \frac{[2s(1-s)]^{\frac{p}{2}}}{\sqrt{\pi}} \Gamma\left(\frac{1+p}{2}\right) \quad (35)$$

$$= \sqrt{\frac{2^p}{\pi}} \frac{\Gamma^2\left(\frac{p}{2} + 1\right)}{\Gamma(p+2)} \Gamma\left(\frac{1+p}{2}\right) \quad (36)$$

$$= \sqrt{\frac{2^{-p}}{\pi}} \frac{\Gamma\left(\frac{p}{2} + 1\right)}{p+1} \quad (37)$$

for  $p > 1$ , so that, in particular, for  $p = 2$  we get

$$L^{-1} E_{\text{opt}} \rightarrow \int_0^1 ds s(1-s) = \frac{1}{6}. \quad (38)$$

Now, let us consider two intermediate times,  $s$  and  $t$ , with  $0 < s < t < 1$  (see again Fig. 6). The probability that the process started at the origin arrives at  $x_1$  after a time  $s$  is that of a Wiener process, so that it is a Gaussian with zero mean and variance  $s$ :

$$p_{W(s)}(x_1) = \frac{1}{\sqrt{2\pi s}} e^{-\frac{x_1^2}{2s}}. \quad (39)$$

Similarly, to move from  $x_1$  to  $x_2$  in the interval  $(t-s)$ :

$$p_{W(t-s)}(x_2 - x_1) = \frac{1}{\sqrt{2\pi(t-s)}} e^{-\frac{(x_2-x_1)^2}{2(t-s)}} \quad (40)$$

and, finally, to move from  $x_2$  to 0 in the interval  $(1-t)$ :

$$p_{W(1-t)}(x_2) = \frac{1}{\sqrt{2\pi(1-t)}} e^{-\frac{x_2^2}{2(1-t)}}. \quad (41)$$

Since the distribution is Gaussian, which means that the joint distribution has the form (105) discussed in the Appendix

$$p_A(x_1, x_2) = \sqrt{\det A} \frac{e^{-\frac{1}{2} \sum_{i=1}^2 x_i A_{ij} x_j}}{2\pi}, \quad (42)$$

by a change of parameters, if we consider the three segments of length

$$\begin{aligned} a &= s \\ b &= t - s \\ c &= 1 - t, \end{aligned} \quad (43)$$

we get that the matrix  $A$  is given by

$$A = \begin{pmatrix} \frac{1}{a} + \frac{1}{b} & -\frac{1}{b} \\ -\frac{1}{b} & \frac{1}{c} + \frac{1}{b} \end{pmatrix}. \quad (44)$$

with

$$\det A = \frac{a + b + c}{abc}. \quad (45)$$

Let us now investigate the correlation function. Given the continuous variable

$$\sigma(s) := \frac{\varphi(s)}{|\varphi(s)|} = \text{sgn}(\varphi(s)) \quad (46)$$

for  $s \in [0, 1]$ , we shall look at the correlation function

$$G(s, t) = \langle \sigma(s)\sigma(t) \rangle = \langle \text{sgn}(\varphi(s)\varphi(t)) \rangle. \quad (47)$$

Let us assume  $s < t$ , rename  $s = a$  and  $t = a + b$ , and use  $c$  as a synonym of  $1 - a - b$ . We can study the slightly more general quantity, function of  $a$ ,  $b$  and  $c$  with no constraint  $a + b + c = 1$

$$\begin{aligned} G(a, b, c) &= \iint dx dy p_A(x, y) \text{sgn}(x \cdot y) \\ &= \iint dx dy \sqrt{2\pi} \sqrt{a + b + c} \frac{e^{-\frac{x^2}{2a} - \frac{(x-y)^2}{2b} - \frac{y^2}{2c}}}{\sqrt{2\pi a} \sqrt{2\pi b} \sqrt{2\pi c}} \text{sgn}(x \cdot y) \end{aligned} \quad (48)$$

If we define

$$\alpha(a, b, c) := \int_{x \geq 0} \int_{y \geq 0} dx dy p_A(x, y) \quad (49)$$

and

$$\beta(a, b, c) := \int_{x \geq 0} \int_{y \leq 0} dx dy p_A(x, y), \quad (50)$$

then

$$G(a, b, c) = 2\alpha(a, b, c) - 2\beta(a, b, c). \quad (51)$$

In addition, since  $p_A(x, y)$  is a normalised Gaussian, we know that

$$2\alpha(a, b, c) + 2\beta(a, b, c) = 1, \quad (52)$$

then

$$G(a, b, c) = 4\alpha(a, b, c) - 1. \quad (53)$$

By performing the integral (49), we find

$$\alpha(a, b, c) = \frac{1}{4} + \frac{1}{2\pi} \arctan \sqrt{\frac{ac}{b(a + b + c)}}, \quad (54)$$

and then

$$G(a, b, c) = \frac{2}{\pi} \arctan \sqrt{\frac{ac}{b(a+b+c)}}. \quad (55)$$

Specialising to  $a + b + c = 1$ , this simplifies to

$$G(a, 1 - a - c, c) = \frac{2}{\pi} \arctan \sqrt{\frac{ac}{1 - a - c}}. \quad (56)$$

If we keep the distance  $b = t - s$  between the two points constant, and we calculate the mean over the interval  $[0, 1]$ , we finally obtain

$$G_{\text{obc}}(b) = \frac{1}{1 - b} \int_0^{1-b} da G(a, b, 1 - a - b) = \frac{1 - \sqrt{b}}{1 + \sqrt{b}}. \quad (57)$$

We found an excellent agreement of the theoretical predictions with the numerical data, even at sizes as small as  $L = 100$ . This can be seen in Fig. 3.

### 3 Periodic boundary conditions

In this section we analyse the one-dimensional Matching Problem with periodic boundary conditions. All along the section, the indices are considered modulo  $L$  (e.g.,  $r_i$  and  $r_{i+L}$  are the same red-point coordinate).

#### 3.1 Properties of the optimal matching

Also in the realisation of the problem with periodic boundary conditions, criticality is obtained when the two sets of points have the same cardinality. However, we no longer have here the trivial characterisation of the optimal solution for  $p > 1$ . We have a result analogous to Proposition 2.1, that is however more subtle and complicated. Again, we compare subconfigurations of candidate solutions, but, differently from the open-boundary case, we need to consider *triples* of points, instead of pairs.

For an ordered triple of points  $(x, y, z)$  on an (oriented) circle, we say that it is *cyclically oriented* if  $x, y$  and  $z$  appear on the circle in (say) counter-clockwise order. Clearly, any other permutation of the three points will be cyclically oriented, or not, depending on the signature of the permutation. For two triples, we say that they are *cyclically co-oriented* if they are oriented in the same direction (clockwise or counter-clockwise).

A maximal matching  $\pi$  is said to be *cyclic* if, for all triples of distinct edges  $(i_1, j_1), (i_2, j_2), (i_3, j_3)$  in  $\pi$ , the two triples  $(i_1, i_2, i_3)$  and  $(j_1, j_2, j_3)$  are cyclically co-oriented.

The following lemma is what we need to obtain a characterization of the solution for the matching problem when  $p \geq 1$ .

**Proposition 3.1** *Consider the matching problem for distinct points on the circle of unit length  $\mathcal{S}^1$  with distance between two points given by the minimal length along the two possible connecting paths. If  $p > 1$ , the optimal matching  $\pi_{\text{opt}}$  is unique and cyclic. If  $p = 1$ , there exists a cyclic optimal matching.*

**Proof.** We proceed by absurd, assuming that an optimal matching  $\pi$  has a triple of edges which are not cyclically co-oriented, and showing that a transposition of two of these edges decreases the cost if  $p > 1$ . The statement for  $p = 1$  then follows by continuity.

Call  $(r_1, r_2, r_3)$  the positions of the three red points, in cyclic order, and  $(b_1, b_2, b_3)$  those of the blue points, also in cyclic order, here given as reals in  $[0, 1)$  and intended modulo 1. The antipodal positions  $(\bar{r}_1, \bar{r}_2, \bar{r}_3)$  and  $(\bar{b}_1, \bar{b}_2, \bar{b}_3)$  are the same lists, shifted by  $\frac{1}{2}$ , and taken modulo 1. This makes 12 points on the circle, say for simplicity all distinct, and 12 intervals (the case of points at antipodes corresponds to the limit of some interval having zero length, that just simplifies the treatment).

Such a structure is equivalently encoded by an ordered 12-tuple  $(x_1, \dots, x_{12})$  of elements in  $[0, 1)$ , such that  $x_{i+6} = x_i + \frac{1}{2}$ , and by a string of 12 elements in  $\{\text{red, blue, white}\}$  such that red and blue have three preimages (here white stands for antipodal, regardless from the colour of the antipode). We call such a string a *pattern*, and denote by  $(a_1, a_2, \dots, a_6)$  the lengths of the intervals, i.e.  $(x_2 - x_1, x_3 - x_2, \dots, \frac{1}{2} + x_1 - x_6)$ . These parameters are subject to  $a_1 + \dots + a_6 = \frac{1}{2}$ , but, given the homogeneity of the cost function, we can safely ignore this constraint.

We can assume, without loss of generality, that the first of the 12 points is a red point, i.e. restrict to patterns starting with “red”. This makes  $320 = \binom{5}{2} 2^5$  possible patterns. Using the  $D_3$  dihedral symmetry of the problem at hand, this can be reduced to  $72^3$ .

The reason for considering the antipodal points is the fact that the distance is given by an “if” condition, on the lengths of the two paths. Once the antipodes are taken into account, we see that the two paths have length of the form  $a_l + \dots + a_{l+s}$  and  $a_l + a_{l+s} + 2a_{l+s+1} + \dots + 2a_{l+6}$  (all the indices are modulo 6), for  $1 \leq s \leq 5$  and  $1 \leq l \leq 6$ , and the “if” statement trivialises. So, for a given pattern, all the 9 relevant distances from  $r_i$  to  $b_j$  are easily determined, simultaneously for all choice of non-negative parameters  $\{a_l\}$ .

The comparison of distinct permutations is made a bit simpler by the fact that two permutations with opposite signature in  $\mathfrak{S}_3$  always differ by a simple transposition, so that one expression is in common.

---

<sup>3</sup>That is slightly more than  $320/6$ , due to the fact that we save less by symmetry for configurations having a non-trivial group of automorphisms.

What we manage to prove is something slightly stronger than the claim in the proposition. Namely, not only we prove that, for all patterns  $P$ , non-cyclic permutations  $\{(132), (213), (321)\}$ , and choice of parameters  $\{a_l\}$ , there exists a cyclic permutation in  $\{(123), (231), (312)\}$  of lower cost, but also that the choice of such cyclic permutation can be made uniform for a given pattern, regardless of the non-negative values of the  $\{a_l\}$ 's. Furthermore, when comparing a cyclic and a non-cyclic permutation, the bound occurs through two mechanisms only.

- One or more variable  $a_l$  does not appear in the two non-common expressions for the distances in the cyclic permutation, while it appears in the expressions for the distances in the non-cyclic one. If these variables are set to zero, the three expressions for the distances become identical in the two permutations.
- Possibly after setting some variables to zero as in the previous case, the two non-common expressions take the form  $\{A + B, B + C\}$ , for the cyclic permutation, and  $\{A + B + C, B\}$ , for the non-cyclic one. Then, the cyclic permutation has a lower cost because  $(1 + x)^p + (1 + y)^p < 1 + (1 + x + y)^p$  for all  $p > 1$  and  $x, y > 0$ .

The second mechanism is compatible with the emergence of degeneration of the optimal solution at  $p = 1$ , as in this case, of course,  $(1 + x) + (1 + y) = 1 + (1 + x + y)$ .

We successfully checked the 72 patterns, and three non-cyclic permutations per pattern, by computer, under the ansatz that the bound was of one of the two forms above.

Just to give an example, consider the pattern  $[\bullet \cdot \cdot \cdot \bullet \circ \cdot \bullet \circ \circ \cdot \cdot]$  (where we used  $\bullet$ ,  $\circ$  and  $\cdot$  for red, blue and white, respectively), and just call  $a, b, \dots, f$  the parameters  $a_l$ . We have

	cyclic		non-cyclic
123	$a + b + c + d + e$ $e + f + a + b$ $b + c$	132	$a + b + c + d + e$ $e + f + a + b + c$ $b$
231	$c + d + e + f$ $e + f + a + b + c$ $f + a$	213	$c + d + e + f$ $e$ $b + c$
312	$d + e + f$ $e$ $b$	321	$d + e + f$ $e + f + a + b$ $f + a$

The non-cyclic permutation (213) is bounded by (312), as  $c$  does not appear in the expressions for the latter, and, after setting  $c \rightarrow 0$ , the two unordered lists of expressions do coincide, thus the first criterium applies.

The non-cyclic permutation (132) is bounded by (123), as the first expressions coincide, and the two remaining ones have the form  $(A + B + C, B, A + B, B + C)$  with  $B = b$ , and  $\{A, C\} = \{e + f + a, c\}$ , thus the second criterium applies.

The non-cyclic permutation (321) is bounded by (312), as the first expressions coincide, and, for the two remaining ones, after setting  $f = a = 0$ , we have the form  $(A + B + C, B, A + B, B + C)$  with  $B = 0$ , and  $\{A, C\} = \{b, e\}$ , thus the second criterium applies.

As mentioned above, all the other patterns are treated similarly.  $\square$

**Proposition 3.2** *When  $|\mathcal{R}| = |\mathcal{B}| = L$ , the cyclic maximal matchings are all and only the permutations of the form  $(i, i + 1, \dots, L, 1, 2, \dots, i - 1)$ .*

**Proof.** Let  $i \neq j$ . Either  $\pi(i) - \pi(j) = i - j$  modulo  $L$  for all pairs, or there exists at least one pair of indices  $i$  and  $j$  such that  $\pi(i) - \pi(j) \neq i - j$  modulo  $L$ . In the second case, consider the interval  $I = (i, i + 1, \dots, j)$  and  $J = (\pi(i), \pi(i) + 1, \dots, \pi(j))$ . As these intervals have different cardinality, there must exist a  $k$  such that either  $k \in I$  and  $\pi(k) \notin J$  or  $k \notin I$  and  $\pi(k) \in J$ . Therefore the triples  $(i, j, k)$  and  $(\pi(i), \pi(j), \pi(k))$  are not cyclically co-oriented.  $\square$

This means that, if we label the points in the sets  $\mathcal{R}$  and  $\mathcal{B}$  in increasing counter-clockwise order, in the unique optimal solution (for  $p > 1$ , or one optimal solution, for  $p = 1$ ) our function  $\phi_i$  has the form

$$\varphi_i = b_i - r_{i-\ell} \tag{58}$$

with a particular  $\ell \in \{0, \dots, L - 1\}$ .

## 3.2 Numerical results

In Fig. 7 we report the correlation function  $G(r; L, t)$  for various choices of the parameter  $t$  when the size of the system is  $L = 6000$ . Each curve is the mean over  $10^3$  instances. The function is even under the parity  $r \rightarrow L - r$  so that we plot it only in the interval  $[0, L/2]$ . The function  $G(r; L, t)$  still presents two ranges of behaviour. If  $|t| < \bar{t}(L)$ , with  $\bar{t}(6000) \approx 0.01$ , the function is decreasing with  $r$ , and has, therefore, a minimum at  $r = \frac{L}{2}$ . However, contrarily to the case of open boundary conditions, this is no longer positive definite. When  $|t| > \bar{t}(L)$ , the shape is different. It reaches a minimum at an intermediate value  $r'$ , then goes up again approaching zero as  $r \rightarrow \frac{L}{2}$ .

In Fig. 8 we show the correlation functions at criticality for various sizes. Each numerical point has been obtained by using  $10^4$  instances for the positions of the blue points. Again, all curves collapse under the simple rescaling  $r \rightarrow r/L$ .

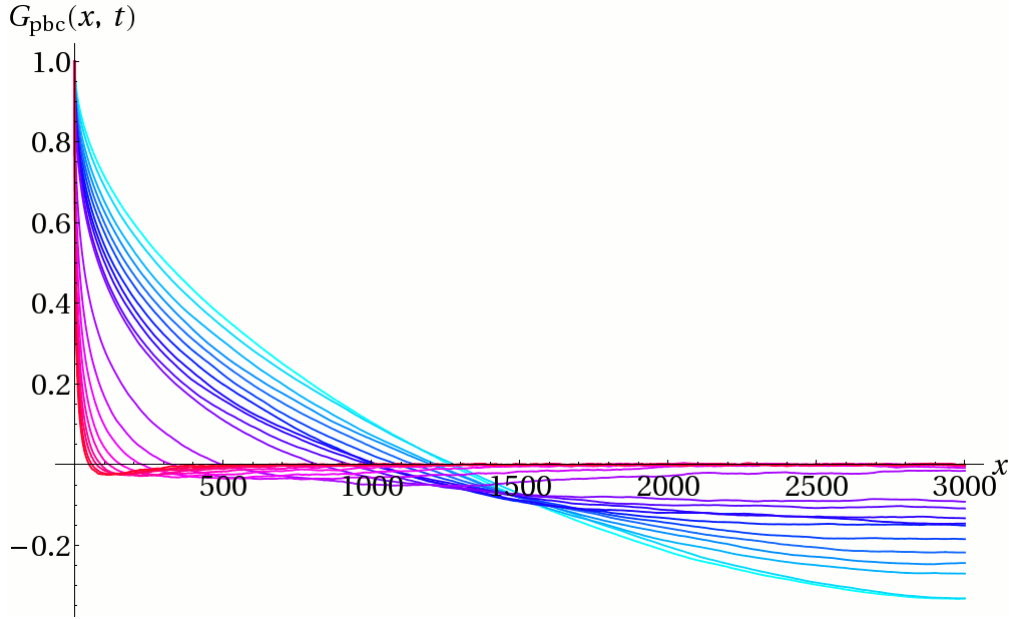


Figure 7: The correlation function near the critical point at size 6000 with periodic boundary conditions for the case  $p = 2$ . From cyan to purple,  $t = 0, 0.001, 0.002, 0.003, 0.004, 0.005, 0.006, 0.007, 0.008, 0.009, 0.01, 0.02, 0.03, 0.04, 0.05, 0.06, 0.07, 0.08, 0.09, 0.1$ .

When  $|t| < \bar{t}(L)$ , if we define  $\bar{x}_L$  as the point where the curve for the size  $L$  has a zero, we find that  $\bar{x}_L(t)$  has a maximum at criticality  $t = 0$  (see Fig. 9). The value of  $\bar{x}_L/L$  at criticality as a function of the size  $L$  is almost constant, we get

$$\frac{\bar{x}_L(t = 0)}{L} \approx 0.2117 \pm 0.0004. \quad (59)$$

We have investigated numerically what happens when we change the exponent  $p$  which appears in the cost function, by looking also at the values  $p = 1, 3, 4$ . The shift which determines the optimal solution is in general different from what we have at  $p = 2$ , and this difference has a consequence on the correlation function. We observe however that the relative variation of the curve is quite small. Fig. 10 presents these results. We plot the correlation function at criticality, that is  $t = 0$ , for the size  $L = 5000$ . Each curve is the mean over  $10^3$  instances.

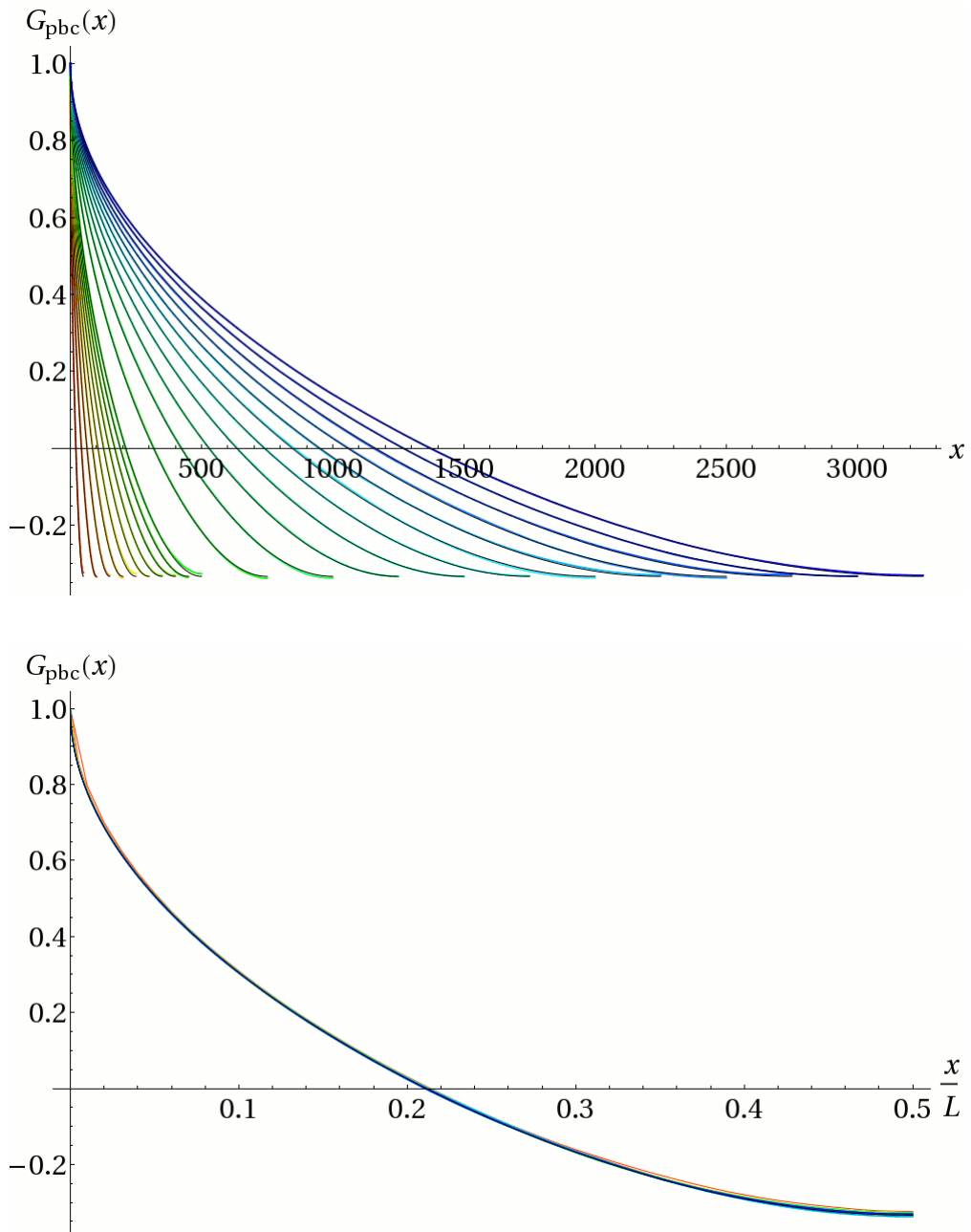


Figure 8: The correlation function with periodic boundary conditions at the critical point for the case  $p = 2$ . Top: increasing sizes are represented from red ( $L = 100$ ) to blue ( $L = 6500$ ); Bottom: the same experimental curves, rescaled to show the agreement with the theoretical function, regardless of the size.

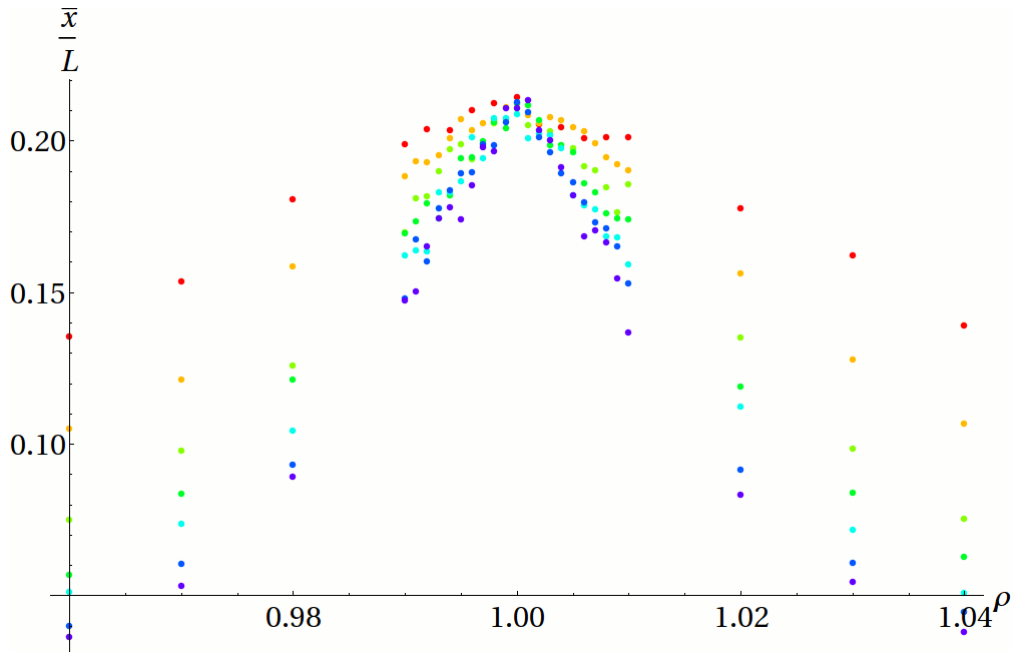


Figure 9: The experimental rescaled intersection with the  $x$ -axis ( $\bar{x}_L/L$ ) as a function of the *reduced temperature*  $t$ . Colours from red to purple for sizes  $L = 500, 1000, 2000, 3000, 4000, 5000, 6000$ .

### 3.3 Analytical predictions at criticality

Recall that the optimal configuration has the structure described in equation (58), i.e. there exists an integer  $\ell$  such that  $\pi_{\text{opt}}(i) = i - \ell$ , and thus  $\varphi_i = b_i - r_{i-\ell}$ . We can define  $\varphi(s)$  analogously to what was done in the previous section, and pass to the continuum limit. Then, after the rescaling with  $L$ , the integer shift  $\ell$  becomes a real variable  $\lambda$ <sup>4</sup> so that our process is a Brownian Bridge, vertically translated by  $\lambda$

$$\varphi_\lambda(s) = B(s) - \lambda \quad (60)$$

By definition, the cost is

$$E[\varphi_\lambda] = \int_0^1 ds |\varphi_\lambda(s)|^p = \int_0^1 ds |B(s) - \lambda|^p. \quad (61)$$

<sup>4</sup>Precisely,  $\lambda \in [-\frac{\sqrt{L}}{2}, \frac{\sqrt{L}}{2}]$ , and the interval converges to  $\mathbb{R}$  in the limit.

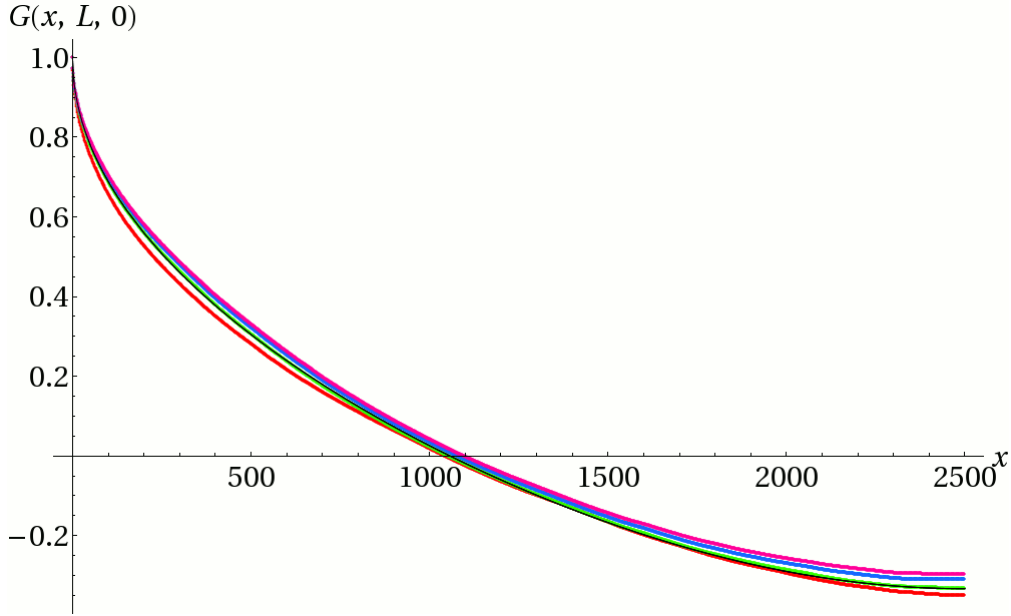


Figure 10: Comparison of the correlation function at criticality, with different values of  $p$  ( $L = 5000$ ). Lines in red, green, blue and purple correspond to  $p = 1, 2, 3, 4$ . The black thinner curve is the plot of the analytic function predicted for  $p = 2$ .

We have a simple necessary condition for optimality, that corresponds to stability w.r.t. the application of an elementary cyclic rotation  $i \rightarrow i \pm 1$

$$\frac{d}{d\lambda} E[\varphi_\lambda] = -p \int_0^1 ds \frac{|\varphi_\lambda(s)|^p}{\varphi_\lambda(s)} = 0. \quad (62)$$

For a fixed configuration of points, this equation is complicated for generic  $p$ . For  $p$  even, it is a real-valued polynomial of degree  $p-1$ , and has in general  $p-1$  roots, and, more precisely,  $2k-1$  real roots and  $\frac{1}{2}p-k$  pairs of complex-conjugate roots. Thus, we have at least one real root, and the global minimum must be achieved at one of these roots. In fact, at generic  $p \geq 1$  the equation has a unique real root, as can be proven by a simple argument. First of all, call  $\mu_B(x)$  the density induced by the Brownian Bridge, i.e.  $\mu_B(x)$  is the derivative of  $\int ds \theta(B(s) - x)$ . Then, the energy reads

$$E[\varphi_\lambda] = \int d\mu_B(x) |x - \lambda|^p, \quad (63)$$

while the stability condition reads

$$\int d\mu_B(x) |x - \lambda|^{p-1} \text{sgn}(x - \lambda) = 0. \quad (64)$$

This equation has always an odd number of real roots. For  $p = 1$ , this is obvious. For  $p > 1$  the asymptotics for  $\lambda \rightarrow \pm\infty$  is  $\sim \pm|\lambda|^{p-1}$ . A further derivative gives

$$-(p-1) \int d\mu_B(x) |x - \lambda|^{p-2} \operatorname{sgn}(x - \lambda)^2 = -(p-1) \int d\mu_B(x) |x - \lambda|^{p-2}, \quad (65)$$

which has definite sign, thus proving the convexity in  $\lambda$  of  $E[\varphi_\lambda]$ . So, the condition (62) is necessary and sufficient for optimality.

When  $p = 2$  this relation is just linear. In this case the optimality condition is trivially solved by

$$\lambda = \int_0^1 ds B(s) \quad (66)$$

It is useful to define the area under the path after time  $t$

$$B^{(-1)}(t) := \int_0^t ds B(s) \quad (67)$$

so that the previous equation just reads  $\lambda = B^{(-1)}(1)$ .

We therefore deduce that our solution converges in the continuum to the process

$$\varphi(s) = B(s) - B^{(-1)}(1) \quad (68)$$

which is a linear combination of the elementary process  $B(s)$ . The value of  $\phi$  at a given coordinate  $s$  is, again, a Gaussian random variable with zero expectation value. The covariance at two coordinates  $(s, t)$  can be easily calculated as follows:

$$\operatorname{cov}[B(s) - B^{(-1)}(1), B(t) - B^{(-1)}(1)] = \frac{1}{12} - \frac{1}{2}t(1-t) - \frac{1}{2}s(1-s) + \min(s, t) - st. \quad (69)$$

If we assume  $s \leq t$ , this expression becomes

$$\operatorname{cov}[\varphi(s), \varphi(t)] = \frac{1}{12} - \frac{1}{2}(t-s)(1-(t-s)), \quad (70)$$

which, as expected, is translational invariant (i.e., depends only on  $t-s$ ) and symmetric w.r.t. reflection (i.e., depends symmetrically on  $t-s$  and  $1-(t-s)$ ). The expression for the covariance satisfies

$$\frac{d^2}{ds^2} \operatorname{cov}[\varphi(s), \varphi(t)] = -\delta(s-t) + 1 \quad (71)$$

where the “+1” correction to the customary  $\delta$ -function is induced by the fact that it shall balance the latter, as, in presence of periodic boundary conditions, the integral of the left-hand side of (71) on the whole interval must vanish.

As a consequence, in the case of periodic boundary conditions, the optimal cost for unit length is

$$L^{-1}E_{\text{opt}} = \frac{1}{12} \quad (72)$$

in agreement with the analysis performed in [16] for the Poisson-Poisson matching, which must differ from this result by a factor two (because of the double contribution to fluctuations, from red and blue points).

If we define

$$\tau = t - s \quad (73)$$

and

$$\eta = \tau(1 - \tau) = (t - s)(1 - (t - s)), \quad (74)$$

the covariance matrix can be written as

$$C = \begin{pmatrix} \frac{1}{12} & \frac{1}{12} - \frac{1}{2}\eta \\ \frac{1}{12} - \frac{1}{2}\eta & \frac{1}{12} \end{pmatrix} \quad (75)$$

and therefore in this case the joint probability distribution is still of the form (105) discussed in the Appendix, now with the matrix  $A$

$$A = C^{-1} = \frac{1}{\eta(1 - 3\eta)} \begin{pmatrix} 1 & -1 + 6\eta \\ -1 + 6\eta & 1 \end{pmatrix}. \quad (76)$$

By comparing (44) with (76), we find

$$\begin{aligned} b &= \frac{\eta(1-3\eta)}{1-6\eta} \\ a + c &= \frac{1-3\eta}{6}. \end{aligned} \quad (77)$$

The important difference with respect to the non-periodic case is that

$$a + b + c = \frac{(1 - 3\eta)^2}{3(1 - 6\eta)}, \quad (78)$$

which is in general  $\neq 1$ . Moreover,  $b$  and  $a + b + c$  can now have a negative sign:

$$\begin{aligned} b &< 0 \\ a + b + c &< 0 \end{aligned} \quad \text{if } \eta > \frac{1}{6}. \quad (79)$$

If  $\eta < \frac{1}{6}$ , the result in (54) is still valid, while if  $\eta > \frac{1}{6}$ , we obtain<sup>5</sup>

$$\alpha(a, b, c) = \frac{1}{2\pi} \arctan \sqrt{\frac{b(a + b + c)}{ac}} \quad (80)$$

$$= \frac{1}{2\pi} \left[ \arctan \left( -\sqrt{\frac{ac}{b(a + b + c)}} \right) + \frac{\pi}{2} \right], \quad (81)$$

---

<sup>5</sup>Here we have used the trigonometric identities:  $\arctan x + \arctan(\frac{1}{x}) = \frac{\pi}{2}$  and  $\arctan(-x) = -\arctan x$ .

which leads to

$$G(\eta) = \begin{cases} \frac{2}{\pi} \arctan \left( \frac{|1-6\eta|}{\sqrt{12\eta(1-3\eta)}} \right) & \text{if } \eta < \frac{1}{6} \\ \frac{2}{\pi} \arctan \left( -\frac{|1-6\eta|}{\sqrt{12\eta(1-3\eta)}} \right) & \text{if } \eta > \frac{1}{6} \end{cases} \\ = \frac{2}{\pi} \arctan \left( \frac{1-6\eta}{\sqrt{12\eta(1-3\eta)}} \right). \quad (82)$$

Or, as a function of  $\tau$ ,

$$G_{\text{pbc}}(\tau) = \frac{2}{\pi} \arctan \left( \frac{1-6\tau(1-\tau)}{\sqrt{12\tau(1-\tau)(1-3\tau(1-\tau))}} \right). \quad (83)$$

Once more we find an excellent agreement with the numerical data, even at sizes as small as  $L = 100$ . This can be seen in Fig. 8.

From the analytic expression (83), we see that the correlation function vanishes when

$$1 - 6\tau(1 - \tau) = 0 \quad (84)$$

that is, at  $\bar{\tau}$  and  $1 - \bar{\tau}$ , with

$$\bar{\tau} = \frac{1}{6} \left( 3 - \sqrt{3} \right) = 0.211325 \dots \quad (85)$$

which coincides with the numerical value given in (59).

## 4 Conclusions

We studied the random one-dimensional Euclidean bipartite matching problem, in which one family of points is on a grid, and the other family is chosen uniformly at random, when the weight function is the power  $p$  of the Euclidean distance.

At criticality, that is when the two set of points have the same cardinality, we can solve the problem exactly, for all  $p > 1$  in the case of open boundary conditions, and for  $p = 2$  in the case of periodic boundary conditions. Besides these exactly-solvable cases, other values of the parameter  $p$ , and the situation in which the two families of points have different cardinality, have been studied numerically.

We have computed the average cost and the two-point correlation function averaged on the distribution of random points. We have verified by a finite-size scaling analysis the existence of a nontrivial continuum limit, when the cardinalities

of the two sets of points are equal and sent to infinity. In this limit a close relation with the Brownian bridge process emerges. In the exactly soluble models we find the values  $\nu = 2$  and  $\alpha = 0$  for the critical exponents which govern the scaling (12).

It would be interesting to understand the tiny changes in the two-point correlation function with  $p > 1$  in the case of periodic boundary conditions.

## Acknowledgements

It is a pleasure to thank Massimiliano Gubinelli for very useful discussions on the continuum limit and Davide Fichera on the Hungarian Algorithm.

S.C. thanks the Université Paris Nord for the support offered to visit LIPN where this work has been finished.

## A Wiener Process and Brownian Bridges

In this appendix we present some standard notions on Brownian Processes, which are used in the paper. For a complete source see for example [21].

### A.1 Wiener process

A standard one-dimensional *Wiener process*, or *Brownian motion process*, is a stochastic process  $W(t)$ :  $t \in \mathbb{R}$ ,  $t \geq 0$ , with the following properties:

- (1)  $W(0) = 0$
- (2) The function  $t \rightarrow W(t)$  is almost surely continuous
- (3) The process  $W(t)$  has stationary, independent increments
- (4) The increment  $W(t) - W(s)$  is normally distributed with expected value 0 and variance  $t - s$

The requirement that  $W(t)$  has *independent increments* means that for all  $t_0 < t_1 < \dots < t_n$ , the  $n$  random variables  $W(t_1) - W(t_0)$ ,  $W(t_2) - W(t_1)$ ,  $\dots$ ,  $W(t_n) - W(t_{n-1})$  are independent. The increments are further said to be *stationary* if, for any  $t > s$  and  $h > 0$ , the distribution of  $W(t + h) - W(s + h)$  is the same as the distribution of  $W(t) - W(s)$ .

## A.2 Basic properties of the Wiener process

- $W(t)$  is a *Gaussian process*, that is for all  $n$  and times  $t_1, \dots, t_n$ , linear combinations of  $W(t_1), \dots, W(t_n)$  are normally distributed

- The unconditional probability density function at a fixed time  $t$  is given by

$$p_{W(t)}(x) = \frac{1}{\sqrt{2\pi t}} e^{-\frac{x^2}{2t}} \quad (86)$$

- $\forall t$ , the expectation is zero:

$$\mathbb{E}[W(t)] = 0 \quad (87)$$

- The variance:

$$\text{var}[W(t)] = \mathbb{E}[W^2(t)] - \mathbb{E}^2[W(t)] = \mathbb{E}[W^2(t)] = t \quad (88)$$

- The covariance<sup>6</sup>:

$$\text{cov}[W(s), W(t)] = \min(s, t) \quad (89)$$

The area of a Gaussian process, defined by

$$W^{(-1)}(t) := \int_0^t ds W(s), \quad (90)$$

is itself a Gaussian process (as a linear combination of Gaussian processes) characterized by its expected value and variance:

$$\mathbb{E}[W^{(-1)}(t)] = \int_0^t ds \mathbb{E}[W(s)] = 0 \quad (91)$$

$$\begin{aligned} \text{var}[W^{(-1)}(t)] &= \mathbb{E} \left[ \int_0^t ds \int_0^t ds' W(s)W(s') \right] = \int_0^t ds \int_0^t ds' \text{cov}(W_s, W_{s'}) \\ &= \int_0^t ds \left( \int_0^s ds' \min(s, s') + \int_s^t ds' \min(s, s') \right) = \frac{t^3}{3}. \end{aligned} \quad (92)$$

---

<sup>6</sup>To see this, let us suppose  $s \leq t$ . Then

$$\begin{aligned} \text{cov}[W(s), W(t)] &= \mathbb{E}[(W(s) - \mathbb{E}[W(s)]) \cdot (W(t) - \mathbb{E}[W(t)])] \\ &= \mathbb{E}[W(s) \cdot W(t)] = \mathbb{E}[W(s) \cdot ((W(t) - W(s)) + W(s))] \\ &= \mathbb{E}[W(s) \cdot (W(t) - W(s))] + \mathbb{E}[W^2(s)] = s \end{aligned}$$

### A.3 Brownian bridge

A standard *Brownian bridge*  $B(t)$  over the interval  $[0, 1]$  is a standard Wiener process conditioned to have  $B(1) = B(0) = 0$ .

Now, if we have a Wiener process  $W(t)$ , the linear combination

$$B(t) := W(t) - tW(1) \tag{93}$$

is a Brownian bridge with expectation, variance and covariance:

$$\mathbb{E}[B(t)] = 0 \tag{94}$$

$$\begin{aligned} \text{var}[B(t)] &= \mathbb{E}[(W(t) - tW(1))^2] \\ &= \mathbb{E}[W^2(t)] - 2t \mathbb{E}[W(1) \cdot W(t)] + t^2 \mathbb{E}[W^2(1)] \\ &= t(1 - t) \end{aligned} \tag{95}$$

$$\begin{aligned} \text{cov}[B(s), B(t)] &= \mathbb{E}[(W(s) - sW(1)) \cdot (W(t) - tW(1))] \\ &= \min(s, t) - st. \end{aligned} \tag{96}$$

This covariance is the Green's function of the second derivative with the given boundary conditions. Indeed,

$$\frac{d^2}{ds^2} \text{cov}[B(s), B(t)] = -\delta(s - t) \tag{97}$$

and this means that the weight of a configuration is

$$W[B] = \exp \left[ - \int_0^1 ds \left( \frac{dB}{ds} \right)^2 \right]. \tag{98}$$

The area of a Brownian bridge, defined by

$$B^{(-1)}(t) := \int_0^t ds B(s), \tag{99}$$

is, again, a Gaussian variable (as a linear combination of Gaussian random variables) characterized by its expected value and variance:

$$\mathbb{E}[B^{(-1)}(t)] = \int_0^t ds \mathbb{E}[B(s)] = 0 \tag{100}$$

$$\begin{aligned}
\text{var}[B^{(-1)}(t)] &= \int_0^t ds \int_0^t ds' \text{cov}[B(s), B(s')] \\
&= \int_0^t ds \int_0^t ds' (\min(s, s') - s s') \\
&= \frac{t^3}{3} - \frac{t^4}{4}.
\end{aligned} \tag{101}$$

In particular, if  $t = 1$ ,

$$\text{var}[B^{(-1)}(1)] = \frac{1}{12} \tag{102}$$

and the covariance between  $B^{(-1)}(1)$  and  $B(t)$  is

$$\begin{aligned}
\text{cov}[B^{(-1)}(1), B(t)] &= \int_0^1 ds \text{cov}[B(s), B(t)] = \int_0^1 ds (\min(s, t) - s t) \\
&= \frac{1}{2} t (1 - t).
\end{aligned} \tag{103}$$

Let us consider the Brownian Bridge  $B$  at two different times,  $B(s)$  and  $B(t)$ , and let us assume that  $s \leq t$ . The covariance matrix is then

$$C = \begin{pmatrix} s(1-s) & s(1-t) \\ s(1-t) & t(1-t) \end{pmatrix}. \tag{104}$$

The distribution is Gaussian, which means the density function is given by

$$p_A(x_1, x_2) = \sqrt{\det A} \frac{e^{-\frac{1}{2} \sum_{i=1}^2 x_i A_{ij} x_j}}{2\pi}, \tag{105}$$

with

$$A = C^{-1} = \begin{pmatrix} \frac{t}{s(t-s)} & -\frac{1}{t-s} \\ -\frac{1}{t-s} & \frac{1-s}{(1-t)(t-s)} \end{pmatrix} \tag{106}$$

## References

- [1] G. Monge, *Mémoire sur la théorie des déblais et des remblais*, in *Histoire de l'Académie Royale des Sciences, Année MDCCLXXXI. Avec les Mémoires de Mathématiques et de Physique pour la même année*, Paris, 1784.
- [2] C. Villani, *Optimal Transport: Old and New*, Grundlehren der Mathematischen Wissenschaften, Springer, 2008.
- [3] H. Kuhn, *The Hungarian Method for the assignment problem*, Naval Research Logistics Quarterly 2, 83–97, 1955.

- [4] D. E. Knuth, *The Stanford GraphBase: A Platform for the Combinatorial computing*, Addison-Wesley, 1993.
- [5] J. Munkres, *Algorithms for the Assignment and Transportation Problems*, J. Soc. Ind. and Appl. Math. 5, 32–38, 1957.
- [6] M. Mézard, G. Parisi, M. A. Virasoro, *Spin Glass Theory and Beyond*, Word Scientific, Singapore, 1987.
- [7] A. K. Hartmann, M. Weigt, *Phase Transitions in Combinatorial Optimization Problems*, John Wiley & Sons, 2006.
- [8] A. Percus, G. Istrate, C. Moore, *Computational Complexity and Statistical Physics*, Oxford University Press, 2006.
- [9] *Complex Systems: Lecture Notes of the Les Houches Summer School 2006*, J.-P. Bouchaud, M. Mézard, J. Dalibard, eds., Elsevier, 2007.
- [10] M. Mézard, A. Montanari, *Information, Physics, and Computation*, Oxford University Press, 2009.
- [11] M. Mézard, G. Parisi, *Mean-Field Equations for the Matching and the Travelling Salesman Problem*, Europhys. Lett. 2, 913–918, 1986.
- [12] M. Mézard, G. Parisi, *On the solution of the random link matching problem*, J. Physique 48, 1451–1459, 1987.
- [13] D. J. Aldous, *The  $\zeta(2)$  limit in the random assignment problem*, Random Structures and Algorithms 18, 381–418, 2001.
- [14] M. Ajtai, J. Komlós and G. Tusnády, *On optimal matchings*, Combinatorica 4, 259–264, 1984.
- [15] A. Holroyd, R. Pemantle, Y. Peres, O. Schramm, *Poisson Matching*, Ann. Inst. Henri Poincaré Probab. Stat. 45, 266–287, 2009 (arXiv:0712.1867).
- [16] S. Caracciolo, C. Lucibello, G. Parisi, G. Sicuro, *A Scaling Hypothesis for the Euclidean Bipartite Matching Problem*, Phys. Rev. E 90, 012118, 2014, (arXiv:1402.6993).
- [17] M. Mézard, G. Parisi, *The Euclidean matching problem*, J. Physique 49, 2019–2015, 1988.
- [18] T. Leighton and P. Shor, *Tight bounds for minimax grid matching with applications to the average case analysis of algorithms*, Combinatorica 9, 161–187, 1989.

- [19] P. W. Shor and J. E. Yukich, *Minimax grid matching and empirical measures*, Ann. Prob. 19, 1338–1348, 1991.
- [20] S. Caracciolo and G. Sicuro, *On the one dimensional Euclidean matching problem: exact solutions, correlation functions and universality*, Phys. Rev. E 90, 042112, 2014, (arXiv:1406.7565).
- [21] R. Durrett, *Probability: Theory and Examples*, 4th Edition, Cambridge University Press, 2010.